

# Accepted Manuscript

Development of acetophenone ligands as potential neuroimaging agents for cholinesterases

Courtney T. Jollymore-Hughes, Ian R. Pottie, Earl Martin, Terrone L. Rosenberry, Sultan Darvesh

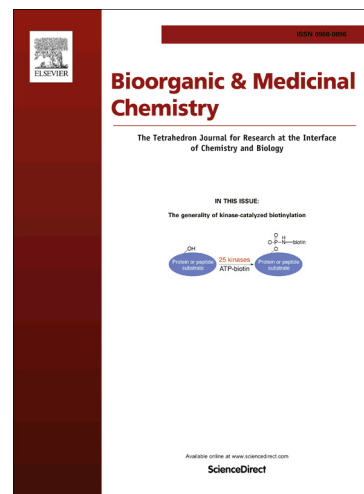
PII: S0968-0896(16)30656-3  
DOI: <http://dx.doi.org/10.1016/j.bmc.2016.08.048>  
Reference: BMC 13231

To appear in: *Bioorganic & Medicinal Chemistry*

Received Date: 18 July 2016  
Revised Date: 22 August 2016  
Accepted Date: 26 August 2016

Please cite this article as: Jollymore-Hughes, C.T., Pottie, I.R., Martin, E., Rosenberry, T.L., Darvesh, S., Development of acetophenone ligands as potential neuroimaging agents for cholinesterases, *Bioorganic & Medicinal Chemistry* (2016), doi: <http://dx.doi.org/10.1016/j.bmc.2016.08.048>

This is a PDF file of an unedited manuscript that has been accepted for publication. As a service to our customers we are providing this early version of the manuscript. The manuscript will undergo copyediting, typesetting, and review of the resulting proof before it is published in its final form. Please note that during the production process errors may be discovered which could affect the content, and all legal disclaimers that apply to the journal pertain.



**Development of acetophenone ligands as potential neuroimaging agents for cholinesterases**

Courtney T. Jollymore-Hughes<sup>a</sup>, Ian R. Pottie<sup>b,c</sup>, Earl Martin<sup>b</sup>, Terrone L. Rosenberry<sup>d</sup>, Sultan Darvesh<sup>a,b, e,\*</sup>

<sup>a</sup>Department of Medical Neuroscience, Dalhousie University, Halifax, Nova Scotia, Canada

<sup>b</sup>Department of Chemistry, Mount Saint Vincent University, Halifax, Nova Scotia, Canada

<sup>c</sup>Department of Chemistry, Saint Mary's University, Halifax, Nova Scotia, Canada

<sup>d</sup>Department of Neuroscience, Mayo Clinic, Jacksonville, Florida, USA

<sup>e</sup>Department of Medicine (Neurology and Geriatric Medicine), Dalhousie University, Halifax, Nova Scotia, Canada

Corresponding Author\*

Sultan Darvesh

Mailing address: Room 1308, Camp Hill Veterans' Memorial Building 1  
5955 Veterans' Memorial Lane, Halifax, Nova Scotia, Canada, B3H 2E1.

Phone: 902-473-2490.

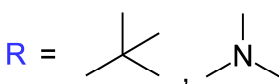
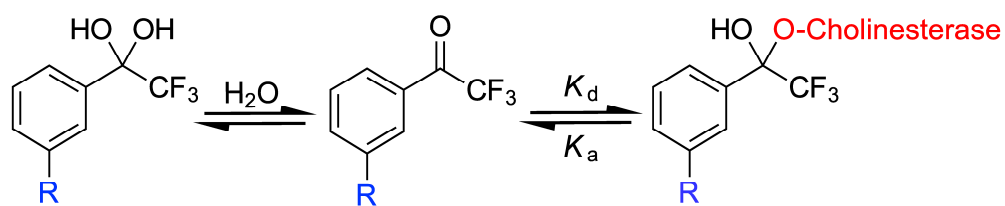
Fax: 902-473-7133.

E-mail: sultan.darvesh@dal.ca.

**ABSTRACT**

Association of cholinesterase with  $\beta$ -amyloid plaques and tau neurofibrillary tangles in Alzheimer's disease offers an opportunity to detect disease pathology during life. Achieving this requires development of radiolabelled cholinesterase ligands with high enzyme affinity. Various fluorinated acetophenone derivatives bind to acetylcholinesterase with high affinity, including 2,2,2-trifluoro-1-(3-dimethylaminophenyl)ethanone (**1**) and 1-(3-*tert*-butylphenyl)-2,2,2-trifluoroethanone (**2**). Such compounds also offer potential for incorporation of radioactive fluorine ( $^{18}\text{F}$ ) for positron emission tomography (PET) imaging of cholinesterases in association with Alzheimer's disease pathology in the living brain. Here we describe the synthesis of two meta-substituted chlorodifluoroacetophenones using a Weinreb amide strategy and their rapid conversion to the corresponding trifluoro derivatives through nucleophilic substitution by fluoride ion, in a reaction amenable to incorporating  $^{18}\text{F}$  for PET imaging. *In vitro* kinetic analysis indicates tight binding of the trifluoro derivatives to cholinesterases. Compound **1** has a  $K_i$  value of 7 nM for acetylcholinesterase and 1300 nM for butyrylcholinesterase while for compound **2** these values are 0.4 nM and 26 nM, respectively. Tight binding of these compounds to cholinesterase encourages their development for PET imaging detection of cholinesterase associated with Alzheimer's disease pathology.

## Graphical Abstract



## Highlights

1. Trifluoroacetophenones have high affinities for cholinesterases
2. Chlorodifluoroacetophenones are suitable precursors for trifluoro derivatives
3. Precursors are rapidly converted to trifluoro analogues via F<sup>-</sup> halogen exchange
4. <sup>18</sup>F incorporation can provide imaging agents for cholinesterases in Alzheimer pathology

## Abbreviations

A $\beta$ :  $\beta$ -amyloid, AD: Alzheimer's disease, AChE: acetylcholinesterase, BuChE:

butyrylcholinesterase, BuLi: butyl lithium, DTNB: 5, 5'-dithiobis 2-nitrobenzoic acid, HPLC:

high performance liquid chromatography, HRMS: high resolution mass spectrum; LRMS: low

resolution mass spectrum, NFTs: neurofibrillary tangles, PET: Positron Emission Tomography,

TMTFA: *m*-(*N,N,N*-trimethylammonium)trifluoroacetophenone.

## Keywords

Cholinesterases, Positron Imaging Tomography, Alzheimer's Disease, Acetylcholinesterase,

Butyrylcholinesterase

## 1. Introduction

Alzheimer's disease (AD) is the most common neurodegenerative disorder that causes dementia.<sup>1</sup> Neuropathological hallmarks of this disease include  $\beta$ -amyloid (A $\beta$ ) plaques and tau neurofibrillary tangles (NFTs)<sup>2</sup> which are required indicators for definitive diagnosis of AD, post-mortem. Since AD can exhibit many clinical symptoms in common with other forms of dementia,<sup>3</sup> it is imperative to develop methods to aid in early definitive diagnosis of AD during life<sup>4</sup> to effect timely treatment of the disease.

Much effort has been devoted to developing imaging agents to detect A $\beta$  in plaques or tau in NFTs.<sup>5-10</sup> Three Positron Emission Tomography (PET) imaging agents were recently approved for use in imaging A $\beta$  deposits but were not approved as specific agents for diagnosing AD<sup>11</sup> because AD pathology can also occur in the brain tissue of up to 30% of cognitively normal older individuals.<sup>12, 13</sup> Therefore, the use of specific A $\beta$  or tau imaging agents could generate many false positive indications of AD<sup>11</sup> and are insufficient for a definitive AD diagnosis during life.<sup>14</sup>

The cholinesterases, acetylcholinesterase (AChE) and butyrylcholinesterase (BuChE), are co-regulators of acetylcholine. These enzymes have been found to co-localize with A $\beta$  plaques that accumulate in various regions of the AD brains, especially in the cerebral cortex.<sup>15-18</sup> In the normal human brain BuChE activity is associated with certain populations of neurons distinct from those with AChE activity.<sup>19-21</sup> In AD, there is an association of cholinesterase activity, particularly that of BuChE, with A $\beta$  plaques.<sup>15-18</sup> Imaging of cholinesterase activity in A $\beta$  plaques<sup>22</sup> has the potential to permit differentiation between such plaques in the brains of cognitively normal older adults from those in AD brains.<sup>16</sup>

Investigations into the distribution of cholinesterases in the brain have been conducted with radiolabelled ligands.<sup>23</sup> A number of  $^{11}\text{C}$  cholinesterase-targeting radioligand substrates have been prepared and tested for the ability to image brain cholinesterase activity. These include *N*- $^{11}\text{C}$ -methylpiperidyl acetate and *N*- $^{11}\text{C}$ -methylpiperidyl propionate<sup>24, 25</sup> for detection of AChE and *N*- $^{11}\text{C}$ -methylpiperidyl butyrate<sup>24, 26-28</sup> for detection of BuChE. However, these agents have yielded only partial recapitulation of known cholinesterase distribution in human brains.<sup>23, 26-28</sup> These substrate-radiotracers, however, have provided proof-of-concept that a sufficient amount survives hydrolysis by cholinesterases in the periphery, cross the blood-brain-barrier, bind to and are hydrolyzed by, cholinesterases to provide PET images through metabolic trapping.<sup>23</sup>

Several cholinesterase inhibitors have also been radiolabelled with  $^{11}\text{C}$  as potential cholinesterase imaging agents. These include  $^{11}\text{C}$ -donepezil,  $^{11}\text{C}$ -methyltacrine, and  $^{11}\text{C}$ -physostigmine, which also have had limited success in demonstrating the known histochemically defined cholinesterase distribution in the brain.<sup>23</sup> Thus, there is a need to develop more effective radioligands that can detect, in the living brain, the distribution of cholinesterases characteristic of AD pathology.

A number of trifluorinated acetophenone derivatives have been shown to be very potent, time-dependent inhibitors of AChE.<sup>29, 30</sup> Foremost among these is *N,N,N*-trimethyl ammonium trifluoroacetophenone (TMTFA), which has very high affinity for AChE.<sup>31</sup> However, this derivative is a quaternary ammonium cation, a property that may represent a possible impediment to crossing the blood-brain barrier for PET imaging cholinesterase activity in the brain. Somewhat less potent neutral trifluoroacetophenones have also been shown to bind to and inhibit AChE<sup>29</sup> and, being uncharged, should cross the blood-brain barrier more readily with estimated LogP values between 2.7 and 3.5. Such  $^{18}\text{F}$ -radiolabelled compounds could potentially

be used for PET imaging of cholinesterase-associated pathology in the living brain.

Radiolabelling of acetophenones has been reported through electrophilic addition using  $^{18}\text{F}$ - $^{19}\text{F}$  gas.<sup>32</sup> The focus of the present work is to develop a generally applicable methodology involving nucleophilic substitution of  $^{18}\text{F}^-$  for chlorine in chlorodifluoro acetophenone derivatives, thereby avoiding the inherent difficulties of handling  $^{18}\text{F}$ - $^{19}\text{F}$  gas. Herein we report the synthesis of *m*-(*N,N*-dimethylamino)trifluoroacetophenone (**1**) and *m*-(*tert*-butyl)trifluoroacetophenone (**2**) and a comparable synthesis of the chlorodifluoro analogues **3** and **4** as precursors for conversion to **1** and **2** by displacement of a chlorine leaving group by  $\text{F}^-$ ,<sup>33</sup> a reaction amenable to incorporation of  $^{18}\text{F}^-$ . Each of the synthesized acetophenones (**1-4**, Figure 1) was tested for its ability to inhibit the enzyme activities of human AChE and BuChE, and all exhibited affinity for both cholinesterases. The reactions of the chlorodifluoromethylketones with AChE have not been reported or quantified previously, and reactions of none of the four compounds with BChE have been previously described. The Weinreb amide strategy for the synthesis of the acetophenone derivatives is consistent with expectations from previous literature reports and represent a valuable practical addition for the preparation of PET tracers. Additional *in vivo* work is beyond the scope of this report but will be conducted in the future.



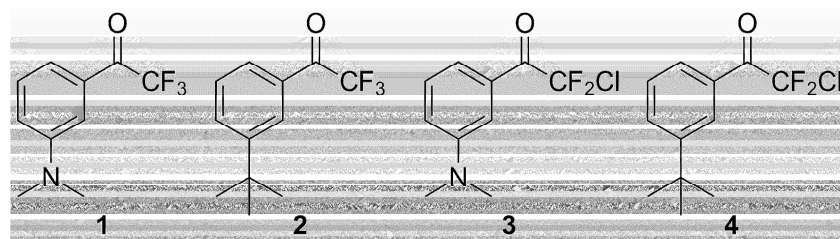
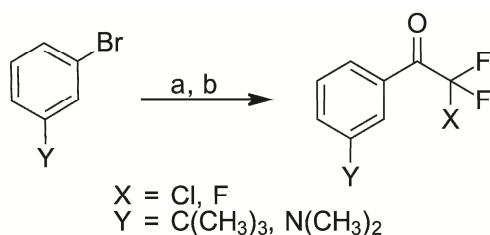


**Figure 1.** Chemical structures of 1-[3-(dimethylamino) phenyl]-2, 2, 2-trifluoroethanone (**1**), 1-(3-*tert*-butylphenyl)-2,2,2-trifluoroethanone (**2**), 1-[3-(dimethylamino) phenyl]-2-chloro-2,2-difluoroethanone (**3**) and 1-(3-*tert*-butylphenyl)-2-chloro-2,2-difluoroethanone (**4**).

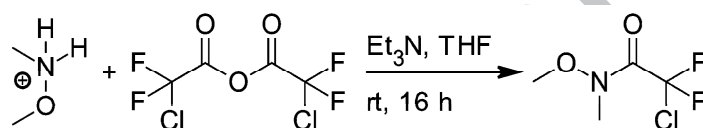
The ability of the trifluoroacetophenones to bind strongly to cholinesterases suggests their potential as PET imaging agents for detecting the association of cholinesterases with AD pathology.

## 2. Results

**2.1. Synthesis of acetophenone derivatives from bromobenzenes.** Four meta-substituted acetophenones (Figure 1), 2,2,2-trifluoro-1-(3-dimethylaminophenyl)ethanone (**1**), 1-(3-*tert*-butylphenyl)-2,2,2-trifluoroethanone (**2**), 2-chloro-2,2-difluoro-1-(3-dimethylaminophenyl)ethanone (**3**) and 2-chloro-2,2-difluoro-1-(3-*tert*-butylphenyl)ethanone (**4**), were synthesized, as outlined in Scheme 1, from a reaction between an organolithium reagent and a Weinreb amide, which was synthesized according to Scheme 2, to generate the desired acetophenone derivatives with non-optimized yields of 42-79%.



**Scheme 1.** Synthesis of *meta*-substituted acetophenones. Reagents and conditions (a) THF,  $-90^\circ\text{C}$ , 1.6M BuLi in hexanes, 15 min (b) For X = F: *N*-methoxy-*N*-methyl-2,2,2-trifluoroacetamide, for X = Cl: *N*-methoxy-*N*-methyl-2-chloro-2,2-difluoroacetamide, 30 min at  $-78^\circ\text{C}$  then  $-78^\circ\text{C}$  to room temperature.

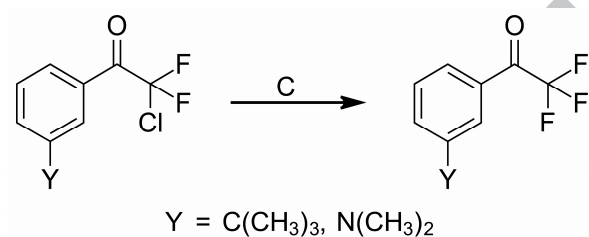


**Scheme 2.** The synthetic strategy to produce *N*-methoxy-*N*-methyl-2-chloro-2,2-difluoroacetamide.

In this method, a *meta*-substituted bromobenzene, having either *m*-dimethylamino or *m*-*tert*-butyl group, was mixed with butyl lithium at  $-90^\circ\text{C}$  to generate the corresponding lithium salt through a halogen-metal exchange reaction. The resulting organolithium reagent was then mixed with either commercially available *N*-methoxy-*N*-methyl-2,2,2-trifluoroacetamide or freshly prepared *N*-methoxy-*N*-methyl-2-chloro-2,2-difluoroacetamide (Scheme 2) to directly give the corresponding products (**1-4**; Figure 1). The chlorodifluoroacetophenones **3** and **4** were found to

have good stability (several weeks) when stored at 5°C in the dark under an atmosphere of anhydrous argon.

**2.2. Conversion of chlorodifluoroacetophenone precursors **3** or **4** to trifluoroacetophenone products **1** or **2**.** We examined the facility with which the chlorodifluoroacetophenones **3** and **4** were converted to the corresponding trifluoroacetophenone products **1** and **2** with a method (Scheme 3) that could be adapted for radiolabelling with nucleophilic  $^{18}\text{F}^-$ .



**Scheme 3.** Conversion of a meta-substituted chlorodifluoroacetophenone to a *meta*-substituted trifluoroacetophenone using a fluorination procedure. Reagents and conditions: (c) KF, Kryptofix<sup>®</sup>, K<sub>2</sub>CO<sub>3</sub>, CH<sub>3</sub>CN, 110°C, 30 min.

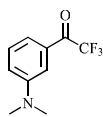
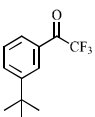
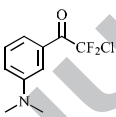
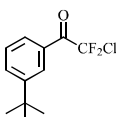
The chlorine atom in compounds **3** and **4** was displaced with fluoride anion to produce a chloride anion and the desired trifluoro compounds by a modification of earlier fluorination reaction procedures.<sup>33, 34</sup> To simulate the process that will be used with radioactive  $^{18}\text{F}^-$ , identical steps were carried out with non-radioactive fluoride ion isotope ( $^{19}\text{F}$ ) as the nucleophilic agent. Production of  $^{18}\text{F}^-$ , generated from bombardment of H<sub>2</sub><sup>18</sup>O in a cyclotron, is subject to

contamination by metal ions. These contaminants are readily removed by chromatographic separation using the Sep-Pak<sup>®</sup> Plus QMA system. In addition, since F<sup>-</sup> is subject to being surrounded by an aqueous solvent shell, which reduces its nucleophilicity, a crown ether, 4,7,13,16,21,24-hexaoxa-1,10-diazabicyclo[8.8.8]hexacosane (Kryptofix<sup>®</sup>), was employed.<sup>33, 34</sup> The Kryptofix<sup>®</sup>/fluoride mixture was then dried by azeotropic distillation with acetonitrile. The dried fluoride reagent was mixed with the chlorodifluoro precursor (**3** or **4**) in anhydrous acetonitrile and the reaction container was sealed with a cap under an atmosphere of argon and heated to 110°C for 30 min for compound **3** and 85°C for 30 min for compound **4**. The product in the cooled reaction mixture was first purified by HPLC, using a C18 reverse phase column, with acetonitrile as the mobile phase (see Materials and Methods). The total time to obtain the purified trifluoro product in this simulated radiolabelling was approximately 60 min. The trifluoro products, obtained from the nucleophilic displacement of the chlorine atom with fluoride ion, using Scheme 3, corresponded to the same compounds obtained from the method outlined in Scheme 1. That is, mass spectral data (Supplementary Figure S25 and S26) for the trifluoro compounds **1** and **2** obtained via Scheme 3 were identical to those for **1** and **2** synthesized via Scheme 1.

**2.3. Inhibition of AChE by acetophenones 1 - 4.** All synthesized acetophenone derivatives were evaluated as potential ligands for human AChE. Although not a focus in this study as potential imaging agents, the precursor chlorodifluoroacetophenones (**3** and **4**) were also examined in order to note any significant differences in structure-activity relationships resulting from the halogen exchange. Previously, a number of fluoroacetophenones have been observed to react with AChE on a time scale of s to min.<sup>29</sup> Therefore, the derivatives prepared here (**1** - **4**,

Scheme 1) were initially examined for any time-dependent reaction with human AChE using a modification<sup>37</sup> of the Ellman method.<sup>38</sup> Three of the four compounds clearly exhibited this type of inhibition of AChE (Table 1).

**Table 1.** Kinetic constants for the interaction of acetophenone-based ligands with acetylcholinesterase<sup>a</sup>

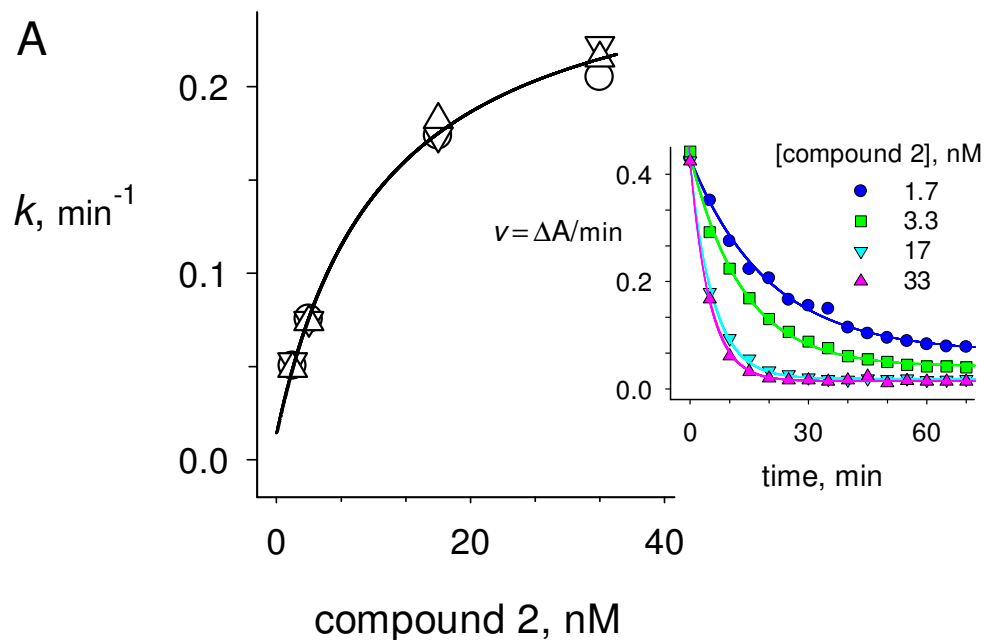
				
	<b>1</b>	<b>2</b>	<b>3</b>	<b>4</b>
$k_a$ ( $\text{nM}^{-1}\text{min}^{-1}$ )	$0.018 \pm 0.021$	$0.024 \pm 0.004^b$	n/a	$0.036 \pm 0.013$
$k_d$ ( $\text{min}^{-1}$ )	$0.36 \pm 0.39$	$0.014 \pm 0.006^b$	n/a	$0.08 \pm 0.08$
$K_i$ (nM) experimental	$7 \pm 2$	$0.4 \pm 0.1$	$42 \pm 7$	$2.9 \pm 0.6$
$K_i$ (nM) calculated as $k_d/k_a$	$20 \pm 31$	$0.56 \pm 0.27^b$	n/a	$2.1 \pm 0.9$

<sup>a</sup>Trifluoro ketones are known to be equilibrium mixtures of the free ketone and the ketone hydrate, and values of  $k_a$  and  $K_i$  can be corrected for hydration.<sup>29</sup> However, no corrections were made here either for hydration or for competition between substrate and inhibitor for the enzyme active site.<sup>29</sup>

<sup>b</sup>Values of  $k_{obs}$  were fitted to Equation 3, and  $k_a$  and  $k_d$  were calculated from Equations 4 – 6.<sup>29</sup>

Enzyme and acetophenone were incubated in 0.1M phosphate buffer (pH 7.4) containing Ellman's reagent; aliquots were removed at set time points up to 70 min, and assays were

initiated with the addition of acetylthiocholine. Assay rate values ( $v$  in  $\Delta A/\text{min}$ ) were plotted against time for several acetophenone concentrations, as illustrated in the Figure 2A inset for compound 2.



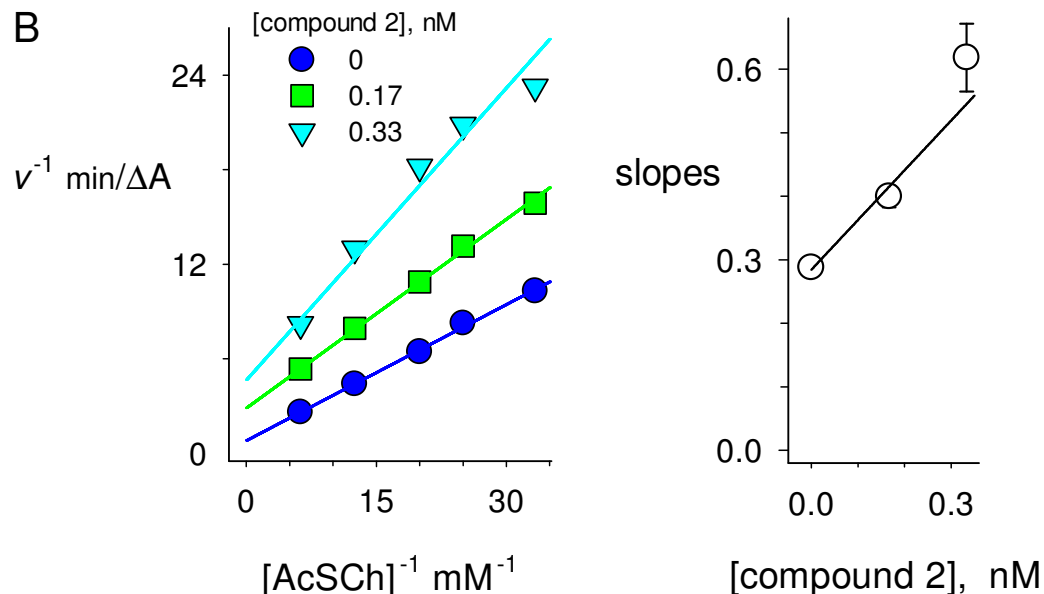
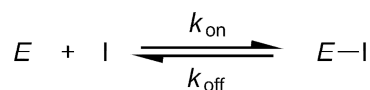


**Figure 2.** Inhibition of AChE by *tert*-butyl trifluoroacetophenone (**2**). A) Time-dependent inhibition is shown by values of  $k_{obs}$  determined by non-linear regression analysis (Equation 2) of the change in enzyme activity ( $v$  in  $\Delta A/\text{dt}$ ) over time for inhibitor concentrations 1.7, 3.3, 17, and 33 nM (inset). Plotting  $k_{obs}$  vs. the concentration of **2** according to Equations 3 – 6 gave the fitted values of  $k_a$  and  $k_d$  shown in Table 1. B) Lineweaver-Burk plots obtained from AChE activities ( $v$ ) at various concentrations of acetylthiocholine substrate ( $[\text{AcSCh}]$ ) and the indicated concentrations of compound **2**. Enzyme and inhibitor were incubated for 30 min before initiating the assays by addition of substrate. Plots of  $1/v$  vs.  $1/[\text{AcSCh}]$  were generated (left panel), and replots of the slopes of these lines against  $[\text{compound 2}]$  (right panel) gave  $K_i$  (see Table 1 for corrected value).

These plots were fitted by nonlinear regression according to Equation 1 to give the pseudo first-order rate constant  $k_{\text{obs}}$ .

$$v = v_f + (v_0 - v_f)\exp(-k_{\text{obs}}t) \quad (1)$$

Previous reports have indicated that replots of  $k_{\text{obs}}$  versus inhibitor concentration are often linear, corresponding to Scheme 4 and Equation 2.<sup>29,31</sup>



**Scheme 4.** Enzyme (E) and Inhibitor (I) interaction showing one equilibrium

$$k_{\text{obs}} = k_{\text{on}}[I] + k_{\text{off}} \quad (2)$$

However, the replots of  $k_{\text{obs}}$  versus inhibitor concentration in this report were all found to be nonlinear, and they could be fitted by Equation 3.

$$k_{\text{obs}} = k_4 + k_3[I]/(K_{21} + [I]) \quad (3)$$

where

$$K_{21} = k_2/k_1 \quad (4)$$

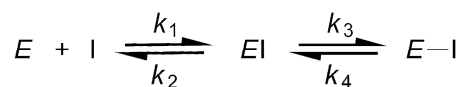
$$k_a = k_3[I]/K_{21} \quad (5)$$

$$k_d = k_3 k_4/(k_3 + k_4) \quad (6)$$

$$K_i = k_d/k_a \quad (7)$$



Equation 3 corresponds to a limiting case of the two-step equilibrium in Scheme 5 in which a rapid initial inhibitor binding is followed by a slower re-equilibration of the complex, as was proposed by Nair et al.,<sup>29</sup> to fit nonlinear replots of  $k_{\text{obs}}$  versus acetophenone concentration.



**Scheme 5.** Enzyme (E) and Inhibitor (I) interaction showing two successive equilibria.

The replot of  $k_{\text{obs}}$  versus the concentration of 2 is shown in Figure 2A, and the nonlinear fit to Equation 3 allowed determination of an overall association rate constant  $k_a = 0.024 \text{ nM}^{-1}\text{min}^{-1}$  and an overall dissociation rate constant  $k_d = 0.014 \text{ min}^{-1}$  from Equations 4 – 6 (see Table 1).

Compounds 1 and 4 also showed time dependent inhibition of AChE, and values of  $k_a$  and  $k_d$  for the reaction of these compounds with AChE were obtained with Equations 3 – 6 and are shown in Table 1. This value of  $k_d$  ( $0.014 \text{ min}^{-1}$ ) corresponds to a half-life of approximately an hour for the complex of compound 2 with AChE, long enough to allow good wash-out of unreacted compound 2 but short enough to avoid toxicity resulting from too much AChE inactivation.

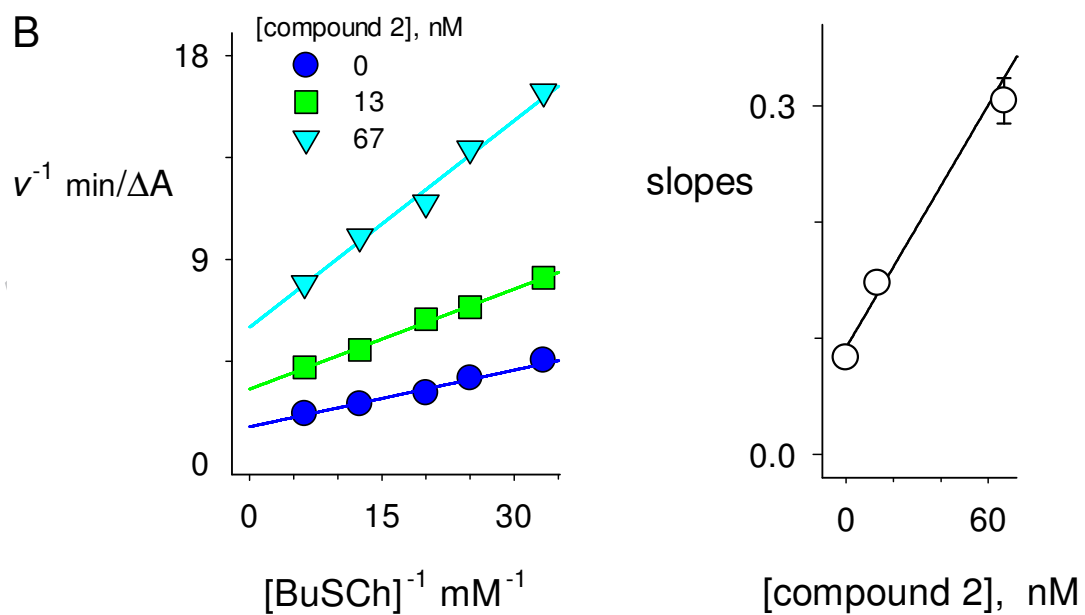
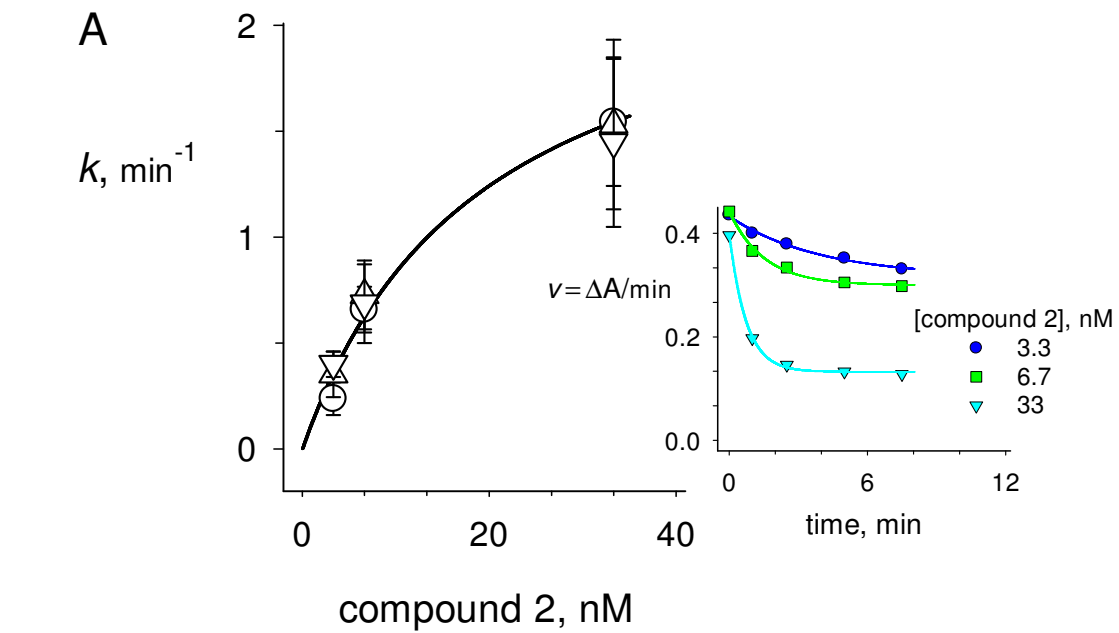
Apparent equilibrium constants  $K_i$  for inhibitor binding to AChE were obtained from steady-state measurements following pre-incubation of enzyme and inhibitor. The analysis is illustrated for compound 2 in Figure 2B. Lineweaver-Burk double reciprocal plots were obtained in the presence and absence of inhibitor. A replot of the slopes of the lines versus inhibitor concentration gave  $K_i$  as the intercept on the x-axis (Table 1,  $K_i$  experimental). Since  $K_i$  is a

measure of the equilibrium dissociation constant of inhibitor and enzyme, a smaller  $K_i$  value indicates a higher affinity for the enzyme. Values of  $K_i$  obtained for the other acetophenones **1**, **3**, and **4** with AChE also are listed in Table 1. The ratio of  $k_d$  to  $k_a$  also should equal  $K_i$  (Equation 7 and see Reference 29), and comparison of this calculated  $K_i$  with that obtained from the steady-state measurements provides an additional check on the consistency of the kinetic data.

$$K_i = k_d/k_a \quad (7)$$

Calculated  $K_i$  values are also shown in Table 1, and their agreement with the experimental  $K_i$  values is within the experimental error.

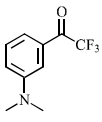
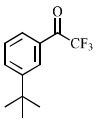
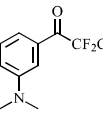
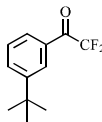
**2.4. Inhibition of BuChE by acetophenones 1 - 4.** Only one of the four acetophenones, compound **2**, showed time-dependent inhibition of BuChE (Figure 3A).



**Figure 3.** Inhibition of BuChE by *tert*-butyl trifluoroacetophenone (**2**). Time-dependent (A) and steady-state inhibition (B) were measured with BuChE and butyrylthiocholine (BuSCh) as in Figure 2 at the indicated concentrations of compound **2** and 15 min preincubation of enzyme and inhibitor. Parameter values are shown in Table 2.

Analytical procedures for the time-dependent and the steady-state assays were as described for AChE except that the substrate butyrylthiocholine was used in place of acetylthiocholine. Results are summarized in Table 2.

**Table 2.** Kinetic constants for the interaction of acetophenone-based ligands with butyrylcholinesterase<sup>a</sup>

	 <b>1</b>	 <b>2</b>	 <b>3</b>	 <b>4</b>
$k_a$ ( $\text{nM}^{-1}\text{min}^{-1}$ )	n/a	$0.13 \pm 0.07^b$	n/a	n/a
$k_d$ ( $\text{min}^{-1}$ )	n/a	$3.4 \pm 2.1^c$	n/a	n/a
$K_i$ (nM) experimental	$1300 \pm 200$	$26 \pm 8$	$1900 \pm 300$	$32 \pm 7$
$K_i$ (nM) calculated as $k_d/k_a$	n/a	n/a	n/a	n/a

<sup>a</sup>Trifluoro ketones are known to be equilibrium mixtures of the free ketone and the ketone hydrate, and values of  $k_a$  and  $K_i$  can be corrected for hydration.<sup>29</sup> However, no corrections were made here either for hydration or for competition between substrate and inhibitor for the enzyme active site.<sup>29</sup>

<sup>b</sup>Values of  $k_{obs}$  were fitted to Equation 3, and  $k_a$  and  $k_d$  were calculated from Equations 4 – 6.<sup>29</sup>

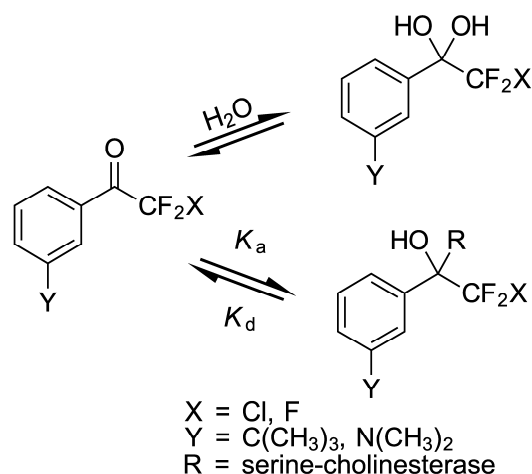
<sup>c</sup>The value of  $k_d$  fitted from Equation 3 was too close to zero to allow an estimate of  $k_d$ . The  $k_d$  shown was calculated from  $k_d = k_a K_i$ , where  $K_i$  was the experimental  $K_i$ .

The  $k_a$  for **2** with BuChE was about five-fold higher than that with AChE, while the calculated  $k_d$  for **2** with BuChE was more than 100-fold larger than that with AChE (Tables 1 and 2). The reversible inhibition constants ( $K_i$ ) obtained from the BChE steady-state data for **2** (Figure 3B) and  $K_i$  values for the other three acetophenones are shown in Table 2. The *tert*-butyl derivatives, **2** and **4**, were the most potent reversible inhibitors of BuChE but the respective  $K_i$  values for all four acetophenones with BuChE were higher than the corresponding  $K_i$  values with AChE, indicating a lower affinity for BuChE. The  $K_i$  for BuChE was 180-fold higher for **1**, 70-fold higher for **2**, 45-fold higher for **3**, and 11-fold higher for **4**, compared to the same values for AChE (Tables 1 and 2).

### 3. Discussion

Current attempts to obtain a definitive diagnosis of AD through specific amyloid neuroimaging fall short since  $\beta$ -amyloid is frequently found in brains of cognitively normal older adults.<sup>12, 13</sup> In contrast, using available neuroimaging techniques to detect the characteristic association of cholinesterases with AD pathology may provide a more definitive diagnosis during life. The development of ligands that bind tightly to cholinesterases and that are also amenable to efficient radiolabelling, with isotopes like  $^{18}\text{F}$  for PET imaging, may offer new opportunities to reveal AD pathology in the living brain and enable more timely diagnosis and monitoring of treatment for the disease. Trifluoroacetophenones are good candidates for such ligands.

Certain acetophenones have been shown<sup>29</sup> to inhibit AChE through covalent interaction between the carbonyl functionality of the ketone inhibitor and the active site serine of the enzyme (Scheme 5).



**Scheme 6.** Hydration and hemiketal equilibria for acetophenone compounds.

This interaction is facilitated by enhancing the electrophilicity of the ketone carbonyl carbon with adjacent electron-withdrawing groups such as a trifluoromethyl group (e.g., Compounds **1** and **2**; Figure 1). Replacement of hydrogen atoms with small electronegative fluorine atoms produces a bioisostere<sup>40</sup> with comparable structure but enhanced ability to form a hemiketal intermediate that blocks substrate access to the enzyme. Trifluoromethyl ketones are known to be potent inhibitors of AChE.<sup>41-43</sup> The nucleophile reacting with the ketone is the activated alkoxide of the catalytic serine residue of the enzyme (Ser203 in human AChE), that results in the formation of the hemiketal-enzyme complex<sup>29</sup> (Scheme 5).<sup>44,45</sup>

The present study sought to determine if chlorodifluoroacetophenones, such as **3** and **4**, were amenable to a radiolabelling methodology to generate potential <sup>18</sup>F imaging agents with high cholinesterase affinity. A number of procedures have been reported<sup>40</sup> for the synthesis of trifluoromethyl ketones, including oxidation of  $\alpha$ -trifluoromethyl alcohols, electrophilic addition

of trifluoroacetic anhydride, alkylation and decarboxylation of fluorinated  $\beta$ -ketoesters or, as described here, through the use of organometallic intermediates. The latter approach (Scheme 1) was chosen as it offered a rapid direct method to obtain the desired *m*-substituted chlorodifluoroacetophenones to be precursors for fluoride exchange reactions. Since the chlorodifluoro derivatives were not commercially available, these were synthesized (Scheme 2) using an organolithium/Weinreb amide strategy. This approach also enabled the direct synthesis of trifluoroacetophenones for proof of identity with the halogen exchange reaction products and for the assessment of cholinesterase affinities (Tables 1 and 2). Due to the relatively short half-life of  $^{18}\text{F}$  ( $t_{1/2} \sim 110$  min), the fluorination reaction to produce the radiolabelled trifluoroacetophenone ligand and all subsequent purification steps must be performed rapidly to maximize the specific activity of the radiolabelled product. It is also important to rapidly separate the desired product from remaining precursor, especially given the structural similarities of the chlorodifluoro precursors and trifluoro products. Purification by C18 reverse phase HPLC allowed for rapid separation of product from the precursor. The halogen exchange reaction with  $^{19}\text{F}$  isotope, and purification, can be performed within one hour and with reasonable yields. Considering time to synthesize and yields, the preparation of trifluoroacetophenone compounds from the chlorodifluoroacetophenone precursors represents a viable method for incorporation of  $^{18}\text{F}$  radioisotope for PET imaging of cholinesterase activity associated with AD pathology. The ability to detect this association by PET imaging is dependent on the affinity of the radioligand for cholinesterase and the length of time it remains in the enzyme-inhibitor hemiketal complex.

Previous studies have mostly focused on the interaction of trifluoromethyl ketones with AChE.<sup>29, 30, 45, 46</sup> Here, BuChE is also considered since it represents a major enzyme component associated with AD pathology.<sup>15-18</sup> Two trifluoroacetophenones, compounds **1** and **2**, were



examined as representative potential radioligands. For comparison, the immediate chlorodifluoro precursors (**3** and **4**, respectively) were also evaluated kinetically for any significant effects on enzyme inhibition due to exchanging halogen species. The ability of fluorinated acetophenones to interact with the catalytic serine of cholinesterases and form a hemiketal complex is indicated by measurable time-dependent inhibition of the enzyme and determined primarily by the magnitude of the first order dissociation rate constant  $k_d$  for the enzyme-inhibitor complex. Lower  $k_d$  values are correlated with higher affinity for enzyme as measured by the experimental  $K_i$  (Table 1) and slower attainment of steady state equilibrium (Scheme 4). *tert*-Butyl trifluoroacetophenone (**2**) showed the highest affinity for AChE, with a  $K_i$  of 0.36 nM (Table 1). Earlier reported  $K_i$  values for **2** with eel and torpedo AChE (1.9 and 3.6 pM, respectively),<sup>29</sup> and mouse AChE (3.7-3.8 pM).<sup>30,47</sup> appear to indicate much higher affinities than that reported here for **2** with human AChE (Table 1). However, typical of most ketones and aldehydes, acetophenones are subject to a hydration equilibrium in aqueous solution (Scheme 4), and these previously reported values were adjusted to take into account the hydration equilibrium constant  $K_{hyd}$  to reflect only the presence of the active ketone form of the molecule.  $K_{hyd}$  has been reported as ~500 for **2**.<sup>30</sup> Before adjustment for  $K_{hyd}$ , the earlier  $K_i$  values for **2** become 0.9 and 1.8 nM with eel and torpedo AChE, respectively, and 1.9 nM for mouse AChE. These values are only slightly higher than the 0.36 nM value in Table 1. Compound **1** also has been reported to show time-dependent inhibition of eel and torpedo AChE with respective  $K_i$  values of 4 nM and 28 nM<sup>29</sup> and of mouse AChE with a  $K_i$  of 15 nM,<sup>30</sup> all prior to correction for hydration, in reasonable agreement with the  $K_i$  value of 7 nM for human AChE in Table 1. The  $K_i$  values reported in Tables 1 and 2 were not adjusted for hydration to better reflect the actual activity of

these molecules in living systems where both the hydrated and nonhydrated forms will be present during imaging studies.

In contrast to AChE, BuChE (Table 2) exhibited a measurable time-dependent inactivation only with compound **2** among the four acetophenones in this study. Values of  $K_i$  obtained from steady-state inhibition of BuChE by all four acetophenones were, as noted in the Results, 10- to 200-fold greater (indicating lower affinity) than those for the same compounds with AChE (Tables 1 and 2).

The three acetophenones that showed time-dependent inhibition of AChE gave association rate constants ( $k_a$ ) in excess of  $10^7 \text{ M}^{-1}\text{min}^{-1}$  (Table 1). The  $k_a$  values for **1** and **2** are within the range of those reported for eel, torpedo, and mouse AChEs.<sup>29,30,47</sup> Only compound **2** provided a measurable  $k_a$  value with BuChE; compounds **1**, **3** and **4** attained steady state equilibrium with BuChE so rapidly that no reaction rate constants could be measured here. The  $k_a$  value of  $13 \times 10^7 \text{ M}^{-1}\text{min}^{-1}$  for **2** with BuChE (Table 2) was five-fold more than the  $k_a$  for **2** with AChE (Table 1), consistent with the larger and more accessible active site gorge in BuChE.<sup>48,49</sup> The observation of a nonlinear dependence of  $k_{\text{obs}}$  on the inhibitor concentration for all of the time-dependent reactions in Tables 1 and 2 indicated that the successive equilibria for acetophenone binding in Scheme 5 and Equations 3 – 6 were more appropriate here than the single equilibrium in Scheme 4 and Equation 2. Scheme 5 and Equations 3 - 6 were invoked previously to account for the binding of compound **1** to eel and torpedo AChE,<sup>29</sup> but it is noteworthy that in that report Scheme 5 and Equation 2 were sufficient to account for the binding of compound **2** to eel or torpedo AChE.<sup>29</sup>

The hemiketal complex formed by acetophenones with cholinesterases is analogous to the tetrahedral transition state intermediate formed during the hydrolysis of ester substrates like

acetylcholine, and enzyme stabilization of this complex promotes catalytic hydrolysis. Since all the acetophenone compounds described here are halogenated methyl ketones, the formation of the hemiketal is likely to be qualitatively similar for all, and this mechanism alone cannot account for the differences in the observed affinities of the derivatives with AChE and BuChE. However, there is a strong correlation between the *meta*-substituent on a trifluoroacetophenone and the potency of its inhibition of AChE. The inhibitor *m*-(*N,N,N*-trimethylammonium)trifluoroacetophenone (TMTFA) has the highest reported affinity of any trifluoroacetophenone with AChE.<sup>29,30</sup> Its  $K_i$  with mouse AChE is 5 fM after correction for hydration and 0.3 nM before correction, values that are nearly 1000-fold higher after correction but only 6-fold higher before correction than those for compound **2** with mouse AChE.<sup>29,47</sup> The high *in vitro* affinity of TMTFA can be attributed largely to a stabilizing cation- $\pi$  interaction between the positively charged nitrogen of the trimethylammonio group with the indole ring of a tryptophan residue (Trp86 in mouse AChE) and, to a lesser extent, to a more electrophilic carbonyl carbon resulting from this electron-withdrawing group.<sup>29</sup> This electrophilic effect could account for the 6- to 8-fold higher affinities of the trifluoroacetophenones **1** and **2** for AChE relative to the corresponding chlorodifluoroacetophenones **3** and **4**, which have less electrophilic carbonyl carbons. In contrast, there are no differences in the affinities of **1** relative to **3** and **2** relative to **4** for BuChE, where hemiketal formation occurs to a lesser extent. Alternatively, these differences may reflect a smaller acyl pocket in the active site of AChE relative to that of BuChE.<sup>48,49</sup>

Tables 1 and 2 indicate that the *m-tert*-butylacetophenones **2** and **4** are 15- to 50-fold more potent reversible inhibitors of both AChE and BuChE than the corresponding *m*-dimethylaminoacetophenones **1** and **3**. It is possible that the lower affinity of the *m*-

dimethylamino derivatives may result from repulsion between the lone pair on the neutral nitrogen atom in the *m*-dimethylamino group of the compound and the indole nitrogen of the corresponding tryptophan residue of human cholinesterases. The absence of such repulsion for compounds **2** and **4** and the larger size of the *tert*-butyl moiety may favour inhibitor stabilization within the active site gorge<sup>29</sup> and help to account for their higher affinities relative to the *m*-dimethylamino acetophenone compounds (**1** or **3**) in our studies.

The absence of an observable time dependence of  $k_{\text{obs}}$  on inhibitor concentration for compound **3** with AChE and compounds **1**, **3** and **4** with BuChE parallels a similar absence of time dependence for some related fluoro ketones with AChE. Nair *et al.*<sup>29</sup> found that trifluoromethyl acetophenones with small *meta*-substituents such as methyl, ethyl, amino or nitro groups did not inhibit AChE in a time-dependent manner but appeared to be reversible inhibitors. They suggested that the larger *meta*-substituents in compounds **1** and **2** can undergo London dispersion interactions in the cholinesterase active site that increase the affinity of trifluoroacetophenones for the enzyme. Such an increase in affinity adds to their appeal as potential imaging agents.

Selective labeling of the target macromolecule is an important goal in neuroimaging. Because of their unique character as tetrahedral transition state analogs of cholinesterases, trifluoroacetophenones should have very high selectivity for AChE and BuChE in the central nervous system. This high selectivity is based on the high affinity of these compounds for the AChE and BuChE active sites, and it is enhanced by the slow dissociation rate constants that several trifluoroacetophenones exhibit with these enzymes. Slow dissociation implies that these compounds will persist in complex with their target molecules during the washout typical of PET imaging analysis. These desirable properties are especially evident in *m-tert*-butyltrifluoroacetophenone (**2**), which exhibits both high affinities (low  $K_i$ s) for the

cholinesterase active sites and a low dissociation rate constant  $k_d$ . These features promise to ensure more selective binding of  $^{18}\text{F}$  labeled acetophenone with cholinesterases associated with AD pathology for PET detection.

#### 4. Conclusion

Two *m*-substituted trifluoroacetophenones, **1** and **2**, have been prepared in a reaction with potential to generate  $^{18}\text{F}$  radioligands for the neuroimaging of cholinesterases associated with AD neuropathology. The precursor molecules of the possible radioligands, *m*-substituted chlorodifluoroacetophenones **3** and **4**, are readily prepared and sufficiently stable to be made in advance and stored for extended periods without chemical degradation. Kinetic evaluations of the trifluoroacetophenones **1** and **2** indicate they bind with high affinity to both AChE and BuChE. The ability to rapidly introduce  $^{19}\text{F}$  by converting **3** to **1** and **4** to **2** indicates that these molecules have potential for development as radioligands for the neuroimaging of cholinesterases and the localization of these enzymes with AD pathology. The present work provides the basis for future studies directed towards incorporation of  $^{18}\text{F}$  into these molecules for PET imaging of cholinesterases in the brain.

#### 5. Materials and Methods

**5.1. Materials and Reagents.** Tetrahydrofuran (HPLC grade, Caledon Labs, CAN) was dried immediately before use in a solvent purification system from Innovative Technology, Newbury Port, MA, USA. Diethyl ether (anhydrous, ACS grade) was used as supplied from Caledon Labs,

CAN. When needed, acetonitrile (HPLC Grade, Caledon Labs, CAN) was dried by refluxing and distilling the solvent over  $\text{CaH}_2$  and immediately used. All other solvents were purchased as HPLC grade and used as supplied from Caledon Labs, CAN. All glassware was dried in an oven at  $110^\circ\text{C}$  for 24 h then cooled to room temperature inside a desiccator before use. 1-Bromo-3-*tert*-butylbenzene was purchased from Oakwood Products, West Columbia, SC, USA. Butyl lithium (1.6M) in hexanes, 3-bromo-*N,N*-dimethylaniline, *N*-methoxy-*N*-methyl-2,2,2-trifluoroacetamide, *N,O*-dimethylhydroxylamine hydrochloride, chlorodifluoroacetic anhydride, sodium sulfate, potassium fluoride, 4,7,13,16,21,24-hexaoxa-1,10-diazabicyclo[8.8.8]hexacosane (Kryptofix<sup>®</sup>), potassium carbonate, acetylthiocholine iodide, *S*-butyrylthiocholine iodide, 5,5'-dithiobis(2-nitrobenzoic acid) and purified recombinant human acetylcholinesterase were purchased from Sigma-Aldrich, USA. Purified human plasma butyrylcholinesterase was a gift from Dr. Oksana Lockridge (University of Nebraska Medical Center). Chemical reactions were performed under ultra-high purity argon or nitrogen atmosphere (Air Liquide, CAN). Sep-Pak<sup>®</sup> Plus QMA (# WAT020545) were purchased from Waters Corp, USA and used as supplied.

**5.2. Characterization of synthesized compounds.** Nuclear magnetic resonance spectra were recorded at the Green Chemistry NMR facility at Saint Mary's University, Halifax, Nova Scotia on a Bruker Avance 300, operating at 300.1 MHz for  $^1\text{H}$  or 75.4 MHz for  $^{13}\text{C}$  experiments; or at the Nuclear Magnetic Resonance Research Resource (NMR-3), Dalhousie University, Halifax, Nova Scotia, Canada on a Bruker AVANCE 500, operating at 500.1 MHz for  $^1\text{H}$  or 125.8 MHz for  $^{13}\text{C}$ . Chemical shifts are reported in parts per million relative to  $\text{Me}_4\text{Si}$  in  $\text{CDCl}_3$ . For  $^1\text{H}$  NMR experiments, the coupling constants are reported in Hertz and the multiplicities are apparent. Infrared spectra were recorded neat between sodium chloride plates on a Nicolet

Avatar 330 FT-IR spectrometer. Peak positions were reproducible within  $1\text{--}2\text{ cm}^{-1}$ . Low-resolution mass spectra (LRMS) were obtained using an Agilent 6890N GC with an Agilent 6890N Electron Impact MS (Waldbronn, Germany) operating at 70 eV. High-resolution mass spectra were obtained with accurate mass positive-ion electrospray ionization or atmospheric-pressure chemical ionization measurements recorded at the Mass Spectrometry Laboratory at Dalhousie University using a Bruker Daltonics microTOF with a flow rate of  $2\text{ }\mu\text{L}/\text{min}$ , spray voltage of 4,500 V and tray temperature of  $180^{\circ}\text{C}$  or were recorded on a CEC 21-110B spectrometer using electron ionization at 70 V and an appropriate source temperature with samples being introduced by means of a heatable port probe. Mass measurements were within 14 ppm of the calculated value. Purity of all compounds was determined using an Agilent Technologies 1200 series HPLC system with a reverse phase C18 column and acetonitrile as the mobile phase. To confirm that compounds **1** and **2** made via Schemes 1 or 3 were identical, an Agilent 6890N gas chromatograph fitted with an HP-5ms column (30 m x 0.255 mm, 0.25 micron coating, Agilent #19091s-433) and a 5973N mass spectrometer operating at 70 eV were used. The GC oven profile was as follows: Initial temperature:  $50^{\circ}\text{C}$  for 3 min, then ramped up by  $20^{\circ}\text{C}$  per minute to  $250^{\circ}\text{C}$  and this temperature was held for 0.5 min. The front inlet profile was as follows: mode: splitless, temperature:  $250^{\circ}\text{C}$ , pressure: 9.78 psi, purge flow: 20.3 mL/min, purge time: 2.00 min, total flow: 24.4 mL/min, gas type: helium. Column profile was as follows: mode: constant flow, average velocity: 40 cm/sec; mass spectrometer transfer line temperature  $200^{\circ}\text{C}$ .

### 5.3. Synthesis of 2,2,2-trifluoro-1-(3-dimethylaminophenyl)ethanone (**1**)

It was prepared as outlined in Scheme 1. In an oven-dried 50 mL round bottom flask under an atmosphere of anhydrous argon, THF (10 mL) was added followed by 3-bromo-*N,N*-dimethylaniline (5.00 mmol, 1.00 g). This clear, colourless solution was cooled to -90°C using a Juablo cooler with a cold finger and an isopropanol bath in an appropriate sized Dewar. The aniline reagent solution was stirred at this temperature for 15 min to ensure the solution was sufficiently cold. Butyl lithium (3.44 mL, 1.60 M in hexanes) was added dropwise at -90°C over 20 min. The resulting clear light yellow solution was stirred for 15 min at -90°C. To this 3-lithium-*N,N*-dimethylaniline intermediate was added *N*-methoxy-*N*-methyl-2,2,2-trifluoroacetamide (5.50 mmol, 0.857 g) dissolved in anhydrous THF (4 mL), dropwise over 15 min. The resulting solution was stirred at -90°C for 30 min then warmed to room temperature by removing the reaction flask from the cooling bath. The resulting reaction mixture was stirred for 16 h at room temperature then extracted with 1M HCl (3 × 10 mL). The combined aqueous layers were added to a separatory funnel and solid NaHCO<sub>3</sub> was added until the solution stopped bubbling. During this addition a yellow liquid formed on the top of the aqueous layer. The aqueous layer was extracted with diethyl ether (3 × 15 mL). The combined organic layers were dried over Na<sub>2</sub>SO<sub>4</sub>, gravity filtered and concentrated *in vacuo*. The crude viscous yellow liquid was purified by flash chromatography on silica gel (5% ethyl acetate/94% hexanes/1% triethylamine, R<sub>f</sub>: 0.38) to afford the desired product as a clear yellow liquid (0.854 g, 79%): <sup>1</sup>H NMR (CDCl<sub>3</sub>): δ 3.02 (s, 6H), 7.02-7.05 (m, 1H), 7.36-7.38 (m, 3H) (Supplementary Figure S1). <sup>13</sup>C-NMR (CDCl<sub>3</sub>): δ 40.0, 112.3, 116.8 (q, *J*<sub>C,F</sub> = 298.2 Hz), 117.9, 119.1, 129.5, 130.4, 150.5, 181.0 (q, *J*<sub>C,F</sub> = 34.3 Hz) (Supplementary Figure S2). IR (Neat): 2898 (m), 2814 (w), 1709 (s), 1600 (s), 1573 (s), 1503 (s), 1437 (m), 1363 (m), 1105 (s), 1007 (s) cm<sup>-1</sup> (Supplementary Figure S3). LRMS *m/z*: 218 (M<sup>+</sup>, 11), 217 (M<sup>+</sup>, 100), 216 (74), 148 (24), 120 (24), 119 (13), 118 (10),



104 (10), 77 (11), 74 (13) (Supplementary Figure S4). HRMS (ESI):  $MH^+$  found 218.0786, calculated for  $C_{10}H_{11}F_3NO^+$  = 218.0787 (Supplementary Figure S5). HPLC: retention time – 2.59 min; purity 96.1% (Supplementary Figure S6).

#### 5.4. Synthesis of 1-(3-*tert*-butylphenyl)-2,2,2-trifluoroethanone (2)

It was prepared as outlined in Scheme 1. In an oven-dried 50 mL round bottom flask under an atmosphere of anhydrous argon, THF (10 mL) was added followed by 1-bromo-3-*tert*-butylbenzene (5.00 mmol, 1.07 g). This clear, colourless solution was cooled to  $-90^\circ\text{C}$  using a Juablo cooler with a cold finger and an isopropanol bath in an appropriate sized Dewar. This solution was stirred at this temperature for 15 min and butyl lithium (3.44 mL, 1.60 M in hexanes) was added dropwise at  $-90^\circ\text{C}$  over 20 min. The resulting clear light yellow solution was stirred for 15 min at  $-90^\circ\text{C}$ . *N*-Methoxy-*N*-methyl-2,2,2-trifluoroacetamide (5.50 mmol, 0.857 g) was dissolved in anhydrous THF (4 mL) then added dropwise to the cooled solution of the above 1-lithium 3-*tert*-butylphenyl intermediate, over 15 min. The resulting solution was stirred at  $-90^\circ\text{C}$  for 30 min then warmed to room temperature by removing the reaction flask from the cooling bath. The resulting reaction mixture was stirred for 16 h at room temperature then quenched with 1M HCl (20 mL). The layers were separated and the aqueous layer was extracted with diethyl ether ( $3 \times 10$  mL). The combined organic layers were dried over  $\text{Na}_2\text{SO}_4$ , gravity filtered and concentrated *in vacuo*. The crude viscous clear liquid was purified by flash chromatography on silica gel (10% ethyl acetate/90% hexanes,  $R_f$ : 0.41) to yield the desired product as a clear, colourless liquid (0.875 g, 76%).  $^1\text{H}$  NMR ( $\text{CDCl}_3$ )<sup>35</sup>:  $\delta$  1.37 (s, 9H), 7.48 (t,  $J=7.9$  Hz, 1H), 7.74-7.77 (m, 1H), 7.86-7.89 (m, 1H), 8.12 (s, 1H) (Supplementary Figure S7).  $^{13}\text{C}$  NMR ( $\text{CDCl}_3$ ):  $\delta$  31.1, 34.9, 116.8 (q,  $J_{C,F} = 291.5$  Hz), 126.8 (q,  $J_{C,F} = 1.6$  Hz), 127.4 (q,

$J_{C,F} = 2.5$  Hz), 128.8, 129.8, 132.8, 152.4, 180.8 (q,  $J_{C,F} = 34.7$  Hz) (Supplementary Figure S8). IR (Neat): 3072 (m), 2966 (s), 2872 (s), 1716 (s), 1600 (s), 1582 (s), 1368 (s), 1156 (s) (Supplementary Figure S9). LRMS  $m/z^{35}$ : 231 ( $M^{+1}$ , 2), 230 ( $M^{+}$ , 13), 216 (14), 215 (100), 187 (50), 161 (18), 118 (10) (Supplementary Figure S10). HRMS (APCI):  $MH^{+}$  found 231.0992, calcd for  $C_{12}H_{14}F_3O^{+} = 231.0991$  (Supplementary Figure S11). HPLC: retention time – 2.18 min; purity 99%; (Supplementary Figure S12).

### 5.5. Synthesis of 2-chloro-2,2-difluoro-1-(3-dimethylaminophenyl)ethanone (3)

It was prepared as outlined in Scheme 1. In an oven-dried 50 mL round bottom flask under an atmosphere of anhydrous argon, THF (10 mL) was added followed by 3-bromo-*N,N*-dimethylaniline (5.00 mmol, 1.00 g). This clear, colourless solution was cooled to  $-90^{\circ}\text{C}$  using a Juablo cooler with a cold finger and an isopropanol bath in an appropriate sized Dewar. The aniline solution was stirred at this temperature for 15 min to ensure the solution was sufficiently cold. Butyl lithium (3.44 mL, 1.60 M in hexanes) was added dropwise at  $-90^{\circ}\text{C}$  over 20 min. The resulting clear light yellow solution was stirred for 15 min at  $-90^{\circ}\text{C}$ . To this 3-lithium-*N,N*-dimethylaniline intermediate was added *N*-methoxy-*N*-methyl-2-chloro-2,2-difluoroacetamide (5, 5.50 mmol, 1.00 g) (see below for synthesis), dissolved in anhydrous THF (4 mL), over 15 min. The resulting solution was stirred at  $-90^{\circ}\text{C}$  for 30 min then warmed to room temperature by removing the reaction flask from the cooling bath. The resulting reaction mixture was stirred for 16 h at room temperature then extracted with 1M HCl ( $3 \times 10$  mL). The combined aqueous layers were added to a separatory funnel and solid  $\text{NaHCO}_3$  was added until the solution stopped bubbling. During this addition a yellow liquid formed on the top of the aqueous layer. The aqueous layer was extracted with diethyl ether ( $3 \times 15$  mL). The combined organic layers were

dried over Na<sub>2</sub>SO<sub>4</sub>, gravity filtered and concentrated *in vacuo*. The crude viscous yellow liquid was purified by flash chromatography on silica gel (5% ethyl acetate/94%hexanes/1%triethylamine, R<sub>f</sub>: 0.37) to yield the desired product as a clear yellow liquid (0.487 g, 42% yield). <sup>1</sup>H NMR (CDCl<sub>3</sub>): δ 3.02 (s, 6H), 7.01-7.03 (m, 1H), 7.36 (t, *J* = 5.0 Hz, 1H), 7.39 (br. S, 1H), 7.44 (d, *J* = 5.0 Hz, 1H) (Supplementary Figure S13). <sup>13</sup>C-NMR (CDCl<sub>3</sub>): δ 40.3, 113.2, 118.4 (t, *J*<sub>C,F</sub> = 3.2 Hz), 118.9, 120.4 (t, *J*<sub>C,F</sub> = 305.2 Hz), 129.3, 130.0, 150.6, 181.9 (t, *J*<sub>C,F</sub> = 28.4 Hz) (Supplementary Figure S14). IR (Neat): 2903 (m), 2812 (m), 1712 (s), 1573(s), 1502 (s), 1436 (s), 1360 (m), 1189 (s), 1144 (s), 880 (w), 800 (w), 678 (s) cm<sup>-1</sup> (Supplementary Figure S15). LRMS m/z: 235 (M<sup>+</sup><sub>2</sub>, 28%), 234 (M<sup>+</sup><sub>1</sub>, 16%), 233 (M<sup>+</sup>, 86%), 232 (18%), 149 (11%), 148 (100%), 120 (73%), 119 (16%), 118 (15%), 105 (20%), 104 (21%), 77 (26%) (Supplementary Figure S16). HRMS (ESI): MH<sup>+</sup> found 234.0497, calcd for C<sub>10</sub>H<sub>11</sub>ClF<sub>2</sub>NO<sup>+</sup>=234.0491 (Supplementary Figure S17). HPLC: retention time – 2.71 min; purity 97% (Supplementary Figure S18).

#### 5.6. Synthesis of 2-chloro-2,2-difluoro-1-(3-tert-butylphenyl)ethanone (4)

It was prepared as outlined in Scheme 1. In an oven-dried 50 mL round bottom flask under an atmosphere of anhydrous argon, THF (10 mL) was added followed by 1-bromo-3-tert-butylbenzene (5.00 mmol, 1.07 g). This clear, colourless solution was cooled to -90°C using a Juablo cooler with a cold finger and an isopropanol bath in an appropriate sized Dewar. This solution was stirred at this temperature for 15 min to ensure it was sufficiently cold. Butyl lithium (3.44 mL, 1.60 M in hexanes) was added dropwise at -90°C over 20 min. The resulting clear light yellow solution was stirred for 15 min at -90°C. *N*-Methoxy-*N*-methyl-2-chloro-2,2-difluoroacetamide (5) (5.50 mmol, 1.00 g), described below, was dissolved in anhydrous THF (4

mL) then added dropwise to the cooled solution of the 1-lithium 3-*tert*-butylphenyl intermediate over 15 min. The resulting solution was stirred at -90°C for 30 min then warmed to room temperature by removing the reaction flask from the cooling bath. The resulting reaction mixture was stirred for 16 h at room temperature then quenched with 1M HCl (20 mL). The layers were separated and the aqueous layer was extracted with diethyl ether (3 × 10 mL). The combined organic layers were dried over Na<sub>2</sub>SO<sub>4</sub>, gravity filtered and concentrated *in vacuo*. The crude viscous clear liquid was purified by flash chromatography on silica gel (10% ethyl acetate/90% hexanes, R<sub>f</sub>: 0.40) to yield the desired product as a clear, colourless liquid (0.629 g, 51%). <sup>1</sup>H NMR (CDCl<sub>3</sub>): δ 1.37 (s, 9H), 7.46 (t, *J* = 7.9 Hz, 1H), 7.71-7.75 (m, 1H), 7.92-7.95 (m, 1H), 8.16 (br s, 1H) (Supplementary Figure S19). <sup>13</sup>C NMR (CDCl<sub>3</sub>): δ 31.1, 35.0, 120.3 (t, *J*<sub>C,F</sub> = 305.1 Hz), 127.5, 127.8 (t, *J*<sub>C,F</sub> = 3.2 Hz), 128.6, 129.2, 132.5, 152.2, 181.5 (t, *J*<sub>C,F</sub> = 28.2 Hz) (Supplementary Figure S20). IR (Neat): 3410 (w), 3072 (m), 2964 (s), 2871 (s), 1713 (s), 1599 (s), 1579 (s), 1367(s), 1162 (s) cm<sup>-1</sup> (Supplementary Figure S21). LRMS *m/z*: 248 (M<sup>+2</sup>, 2%), 247 (M<sup>+1</sup>, 1%), 246 (M<sup>+</sup>, 5%), 233 (17%), 231 (50%), 203 (22%), 162 (13%), 161 (100%), 145 (11%), 118 (12%), 117 (10%), 115 (10%), 91 (11%) (Supplementary Figure S22). HRMS (ESI): MNa<sup>+</sup> found 269.0524, calcd for C<sub>12</sub>H<sub>13</sub>ClF<sub>2</sub>ONa<sup>+</sup>=269.0515 (Supplementary Figure S23). HPLC: Retention time – 2.33 min; purity 98% (Supplementary Figure S24).

### 5.7. Synthesis of N-methoxy-N-methyl-2-chloro-2,2-difluoroacetamide (5)

This reagent was prepared by a modification of the procedure of Tang et al.<sup>36</sup> (Scheme 2). Briefly, *N,O*-dimethylhydroxylamine hydrochloride, (35.9 mmol, 3.50 g) as placed in a 100 mL pear shaped flask that was dried in an oven overnight. The flask was capped with a rubber

septum and flushed with anhydrous argon gas and THF (60 mL) was added.

Chlorodifluoroacetic anhydride (34.1 mmol, 5.94 mL) and triethylamine (35.9 mmol, 5.00 mL) were added sequentially dropwise to the stirring solution. Immediately, the reaction formed a white precipitate. The reaction was stirred for 16 h at room temperature. The reaction was suction filtered through a sintered glass funnel and the filter cake was rinsed with anhydrous diethyl ether. The filtrate was then stirred over  $\text{NaHCO}_3$  (170 mmol, 18.0 g) for 30 min. The mixture was suction filtered and the filtrate was concentrated *in vacuo* at room temperature. The remaining material was vacuum distilled at 60.0 - 60.5°C at 15 mm Hg to afford 4.64 g of the product (78 %) of a clear colourless liquid. IR (neat): 2991 (s), 2949 (s), 1701 (s), 1463 (s), 1395 (s), 1219 (s), 1173 (s), 1081 (s), 996 (s), 958 (s)  $\text{cm}^{-1}$ ;  $^1\text{H}$  NMR : ( $\text{CDCl}_3$ )  $\delta$  3.32 (s, 3H), 3.78 (s, 3H); LRMS : 175 ( $\text{M}^{+2}$ , 7), 174 ( $\text{M}^{+1}$ , 1), 173 ( $\text{M}^{+}$ , 21), 88 (31), 87 (32), 85 (98), 81(67), 60 (71), 59 (10), 58 (100), 56 (22). The  $^1\text{H}$  NMR data for this material was identical to the published data by Tang *et al.*<sup>36</sup>

**5.8. Synthesis of 2,2,2-trifluoro-1-(3-dimethylaminophenyl)ethanone (1) from the 2-chloro-2,2-difluoro-1-(3-dimethylaminophenyl)ethanone (3) or 1-(3-tert-butylphenyl)-2,2,2-trifluoroethanone (2) from the 2-chloro-2,2-difluoro-1-(3-tert-butylphenyl)ethanone (4).**

The following procedure for the incorporation (Scheme 3) of non-radioactive fluoride into precursor compounds **3** and **4** was adapted from previously described methods.<sup>33</sup> This procedure was carried out with “cold”  $^{19}\text{F}$  to simulate the use of radioactive  $^{18}\text{F}$ , which will require removal of cyclotron-generated impurities accumulated during its production, and to provide fluoride ion reagent free of aqueous solvent shell to facilitate nucleophilicity of this anion.<sup>8, 33, 34</sup>

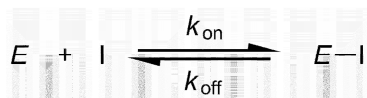
Briefly, KF (4.8 mg, 0.083 mmol) was dissolved in distilled H<sub>2</sub>O (1 mL) and this solution was passed through Sep-Pak<sup>®</sup> Plus QMA. Anhydrous argon gas was then blown through this Sep-Pak<sup>®</sup> for 20 min. At this time, a solution that consisted of Kryptofix<sup>®</sup> (9.5 mg, 0.025 mmol), K<sub>2</sub>CO<sub>3</sub> (4.7 mg, 0.034 mmol), and 5 mL of 17% water/83% acetonitrile was passed through the argon-dried Sep-Pak<sup>®</sup>. The eluent was evaporated to dryness by heating it to 110°C and blowing anhydrous argon over the solution. Anhydrous acetonitrile (2 mL) was then added to the vial and evaporated to dryness by blowing anhydrous argon gas over the solution at 110°C. This acetonitrile addition and evaporation process was repeated two more times to ensure azeotropic removal of all the water. To the dried Kryptofix<sup>®</sup>/KF material was added the chlorodifluoro compound **3** or **4** (0.013 mmol) dissolved in anhydrous acetonitrile (1.0 mL) under an atmosphere of anhydrous argon. The resulting solution was sealed with a cap and heated at 110°C for compound **3** and 85°C for compound **4**, for 30 min. The product was purified by injecting the reaction mixture into a 1200 series Agilent HPLC equipped with a reverse phase C18 column (4.6 x 150mm, Eclipse XDB-C18; mobile phase acetonitrile at 0.3 mL/min for compound **3** and 0.5 mL/min for compound **4**). The peak fraction for each product was collected using Agilent 1200 series fraction collector (G1364C). The product fraction was injected into an Agilent 6890N GC (G1530N) that was equipped with an electron impact 5973 mass selective detector (G2577A) running at 70 eV. The mass spectra of the products **1** (Figure S4) or **2** (Figure S10), synthesized directly according to Scheme 1, corresponded to the mass spectra of **1** or **2** synthesized via the dichloro intermediates (**3** or **4**) according to Scheme 3 (Supplementary Figures S25 and S26, respectively).

### 5.9. Cholinesterase inhibition by acetophenone derivatives

All acetophenone derivatives (**1-4**), were evaluated for their ability to inhibit human AChE and BuChE using a modification<sup>37</sup> of Ellman's method<sup>38</sup> on a Milton-Roy 1201 UV-visible spectrophotometer (Milton-Roy, Ivyland, PA) set at 412nm. To determine time-dependent inhibition, mixtures were prepared with 6.75 mL 5, 5'-dithiobis 2-nitrobenzoic acid (DTNB, 0.36 mM) in 0.1M sodium phosphate buffer (pH 7.4), 0.25 mL of acetonitrile or ligand in acetonitrile, and 0.25 mL enzyme (either 0.03 units of human recombinant AChE, or 0.04 units of human plasma BuChE, in 0.1% aqueous gelatin containing 0.01% sodium azide, where 0.1 unit is taken as the amount of enzyme giving 1.0  $\Delta A/\text{min}$  under standard assay conditions. For incubations of 30 min or longer, bovine serum albumin was also added at 0.1 mg/mL. From the mixture, 1.45 mL aliquots were transferred to a cuvette at 1, 2.5, 5 and 7.5 min for **1** and **3**, or every five min until 70 min for **2** and **4**. Prior to addition of substrate, absorbance of the assay mixture was adjusted to zero absorbance at 412 nm. Assays were initiated by addition of 0.05 mL of substrate (either acetylthiocholine for AChE or butyrylthiocholine for BuChE) to give a final substrate concentration of 5 mM, mixed by inversion and the absorbance monitored every 5 s for 1 minute after an initial 5 second delay to give values of the hydrolysis rates  $v$  as  $\Delta A/\text{min}$ . A zero time point was also obtained by initiating the reaction with enzyme added last after the mixing of ligand and substrate in buffered DTNB. Experiments were done in triplicate at 23°C. Values of  $v$  were fitted to Equation 1, where  $v_f$  is the final rate and  $v_0$  is the rate at time 0, to obtain  $k_{\text{obs}}$ .

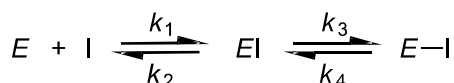
$$v = v_f + (v_0 - v_f)\exp(-k_{\text{obs}}t) \quad (1)$$

Values of  $k_{\text{obs}}$  were fitted to Equations 2 and 3 corresponding to Schemes 4 and 5, respectively.



**Scheme 4.** Enzyme (E) and Inhibitor (I) interaction showing one equilibrium.

$$k_{\text{obs}} = k_{\text{on}}[I] + k_{\text{off}} \quad (2)$$



**Scheme 5.** Enzyme (E) and Inhibitor (I) interaction showing two successive equilibria.

$$k_{\text{obs}} = k_4 + k_3[I]/(K_{21} + [I]) \quad (3)$$

where

$$K_{21} = k_2/k_1 \quad (4)$$

$$k_a = k_3[I]/K_{21} \quad (5)$$

$$k_d = k_3 k_4/(k_3 + k_4) \quad (6)$$

$$K_i = k_d/k_a \quad (7)$$

However, since better fits were obtained with Equation 3, only values of the association rate constant ( $k_a$ ) and the dissociation constant ( $k_d$ ) obtained from Equations 4 – 7 are reported here.

To determine reversible equilibrium inhibition constants ( $K_i$ ) under final steady-state conditions, hydrolysis rates  $v$  were obtained with Ellman assays and analyzed with Lineweaver-Burk plots. The time-dependent assays above established whether final steady states were



obtained within a few s or required longer incubations, but to be certain steady state was reached all steady-state inhibition assays here involved incubations of at least 15 min. An appropriate range of inhibitor concentrations was determined in preliminary experiments with serial dilutions (1:10) of each compound from a 5 mM stock in acetonitrile. Triplicate incubation mixtures were then set up with 24.3 mL of 0.36 mM DTNB in 0.1 M sodium phosphate buffer (pH 7.4), 0.9 mL of enzyme (either 0.03 units of human recombinant AChE, or 0.04 units of human plasma BuChE), and 0.9 mL of acetonitrile (no inhibitor) or 0.9 mL of acetophenone derivative in acetonitrile. Aliquots (1.45 mL) were mixed with 0.05 mL of substrate (acetylthiocholine for AChE or butyrylthiocholine for BuChE) at final concentrations of 0.03 to 0.16 mM, and hydrolysis rates  $v$  were measured at 23°C over a 1 minute period with readings every 5 s.  $K_i$  values for the acetophenone derivatives were obtained by fitting Lineweaver-Burk double reciprocal plots of  $1/v$  vs.  $1/[S]$  (Equation 8), where  $K_{app}$  is the apparent Michaelis constant and  $K_{Si}$  is the apparent uncompetitive inhibition constant resulting from inhibitor binding to the  $ES$  complex. The replot of the slopes of the Lineweaver-Burk plots against ligand concentration gave the  $K_i$  value as the intercept on the x-axis (Equation 9).

$$v^{-1} = \frac{1}{V_{max}} \left[ 1 + \frac{[I]}{K_{Si}} + \frac{K_{app} \left( 1 + \frac{[I]}{K_i} \right)}{[S]} \right] \quad (8)$$

$$\text{Slope} = (K_{app}/V_{max})(1 + [I])/K_i \quad (9)$$

The fitting of kinetic data with cholinesterase inhibitors was conducted by nonlinear regression with SigmaPlot (version 12.0), and analyses were either unweighted (Equation 1) or weighted.<sup>39</sup> Points fitted to Equation 8 were weighted assuming that the dependent variable had constant percent error. Points fitted to Equations 3 and 9 were weighted individually (weight = 1/variance of y) when weights ranged widely over the data set and were unweighted when they did not.

### **Acknowledgments**

Canadian Institutes of Health Research (Frederick Banting and Charles Best Canada Graduate Scholarships, MOP-82798, RNS- 117795, MOP-119343), Killam Trusts, Dalhousie Medical Research Foundation Irene MacDonald Sobey Chair in Curative Approaches to Alzheimer's Disease, Ms. Sadie Macleod through the Dalhousie Medical Research Foundation Adopt-A-Researcher Program, the Committee on Research and Publications, Mount Saint Vincent University, the Brain Repair Centre, Nova Scotia Health Research Fund, Nova Scotia Health Research Foundation (MED-MAT-2011-7512), Faculty and Department of Medicine of Dalhousie University, Innovacorp and Dalhousie Medical Research Foundation.

### **Supporting Data.**

The following information can be found in this file: All spectroscopic information, including <sup>1</sup>H and <sup>13</sup>C NMR, IR, Low resolution mass spectrum, higher solution mass spectrum, and HPLC analysis for purity for compounds **1-4**.

## REFERENCES

1. Reitz, C.; Brayne, C.; Mayeux, R. *Nat. Rev. Neurol.* **2011**, *7*, 137-152.
2. Hyman, B. T.; Phelps, C. H.; Beach, T. G.; Bigio, E. H.; Cairns, N. J.; Carrillo, M. C.; Dickson, D. W.; Duyckaerts, C.; Frosch, M. P.; Masliah, E.; Mirra, S. S.; Nelson, P. T.; Schneider, J. A.; Thal, D. R.; Thies, B.; Trojanowski, J. Q.; Vinters, H. V.; Montine, T. J. *Alzheimers Dement.* **2012**, *8*, 1-13.
3. Beach, T. G.; Monsell, S. E.; Phillips, L. E.; Kukull, W. *J. Neuropathol. Exp. Neurol.* **2012**, *71*, 266-273.
4. Risacher, S. L.; Saykin, A. J. *Annu. Rev. Clin. Psychol.* **2013**, *9*, 621-648.
5. Agdeppa, E. D.; Kepe, V.; Liu, J.; Flores-Torres, S.; Satyamurthy, N.; Petric, A.; Cole, G. M.; Small, G. W.; Huang, S.-C.; Barrio, J. R. *J. Neurosci.* **2001**, *21*, RC189.
6. Zhuang, Z.-P.; Kung, M.-P.; Hou, C.; Plossl, K.; Skovronsky, D.; Gur, T. L.; Trojanowski, J. Q.; Lee, V. M. Y.; Kung, H. F. *Nucl. Med. Biol.* **2001**, *28*, 887-894.
7. Mathis, C. A.; Wang, Y.; Holt, D. P.; Huang, G.-F.; Debnath, M. L.; Klunk, W. E. *J. Med. Chem.* **2003**, *46*, 2740-2754.
8. Wong, D. F.; Rosenberg, P. B.; Zhou, Y.; Kumar, A.; Raymont, V.; Ravert, H. T.; Dannals, R. F.; Nandi, A.; Brasic, J. R.; Ye, W.; Hilton, J.; Lyketsos, C.; Kung, H. F.; Joshi, A. D.; Skovronsky, D. M.; Pontecorvo, M. J. *J. Nucl. Med.* **2010**, *51*, 913-920.
9. Barthel, H.; Sabri, O. *J. Alzheimers Dis.* **2011**, *26 Suppl 3*, 117-121.
10. Hatashita, S.; Yamasaki, H.; Suzuki, Y.; Tanaka, K.; Wakebe, D.; Hayakawa, H. *Eur. J. Nucl. Med. Mol. Imaging* **2014**, *41*, 290-300.
11. Villemagne VL. *Ageing Res Rev.* **2016** Jan 28. pii: S1568-1637(16)30005-8. doi: 10.1016/j.arr.2016.01.005.
12. Bennett, D. A.; Schneider, J. A.; Arvanitakis, Z.; Kelly, J. F.; Aggarwal, N. T.; Shah, R. C.; Wilson, R. S. *Neurology* **2006**, *66*, 1837-1844.
13. Aizenstein, H. J.; Nebes, R. D.; Saxton, J. A.; Price, J. C.; Mathis, C. A.; Tsopelas, N. D.; Ziolkowski, S. K.; James, J. A.; Snitz, B. E.; Houck, P. R.; Bi, W.; Cohen, A. D.; Lopresti, B. J.; DeKosky, S. T.; Halligan, E. M.; Klunk, W. E. *Arch. Neurol.* **2008**, *65*, 1509-1517.
14. Kepe, V.; Moghbel, M. C.; Langstrom, B.; Zaidi, H.; Vinters, H. V.; Huang, S.-C.; Satyamurthy, N.; Doudet, D.; Mishani, E.; Cohen, R. M.; Hoiland-Carlson, P. F.; Alavi, A.; Barrio, J. R. *J. Alzheimer's Dis.* **2013**, *36*, 613-631.
15. Friede, R. L. Enzyme histochemical studies of senile plaques. *J. Neuropathol. Exp. Neurol.* **1965**, *24*, 477-491.
16. Mesulam, M. M.; Geula, C. *Ann. Neurol.* **1994**, *36*, 722-727.
17. Guillozet, A. L.; Smiley, J. F.; Mash, D. C.; Mesulam, M. M. *Ann. Neurol.* **1997**, *42*, 909-918.
18. Darvesh, S.; Reid, G. A.; Martin, E. *Curr. Alzheimer Res.* **2010**, *7*, 386-400.
19. Graybiel, A. M.; Ragsdale, C. W., Jr. *Nature* **1982**, *299*, 439-442.
20. Darvesh, S.; Grantham, D. L.; Hopkins, D. A. *J. Comp. Neurol.* **1998**, *393*, 374-390.
21. Darvesh, S.; Hopkins, D. A. *J. Comp. Neurol.* **2003**, *463*, 25-43.
22. Darvesh, S. *Chem.-Biol. Interact.* **2013**, *203*, 354-357.
23. Kikuchi, T.; Okamura, T.; Zhang, M.-R.; Irie, T. *J. Labelled Compd. Radiopharm.* **2013**, *56*, 172-179.

24. Irie, T.; Fukushima, K.; Akimoto, Y.; Tamagami, H.; Nozaki, T. *Nucl. Med. Biol.* **1994**, *21*, 801-808.
25. Kilbourn, M. R.; Snyder, S. E.; Sherman, P. S.; Kuhl, D. E. *Synapse* **1996**, *22*, 123-131.
26. Kikuchi, T.; Fukushima, K.; Ikota, N.; Ueda, T.; Nagatsuka, S.-I.; Arano, Y.; Irie, T. *J. Labelled Compd. Radiopharm.* **2001**, *44*, 31-41.
27. Roivainen, A.; Rinne, J.; Virta, J.; Jaervempaee, T.; Salomaeki, S.; Yu, M.; Nagren, K. *J. Nucl. Med.* **2004**, *45*, 2032-2039.
28. Kuhl, D. E.; Koeppe, R. A.; Snyder, S. E.; Minoshima, S.; Frey, K. A.; Kilbourn, M. R. *Ann. Neurol.* **2006**, *59*, 13-20.
29. Nair, H. K.; Seravalli, J.; Arbuckle, T.; Quinn, D. M. *Biochemistry* **1994**, *33*, 8566-8576.
30. Quinn, D. M.; Feaster, S. R.; Nair, H. K.; Baker, N. A.; Radic, Z.; Taylor, P. J. *Am. Chem. Soc.* **2000**, *122*, 2975-2980.
31. Nair, H. K.; Lee, K.; Quinn, D. M. *J. Am. Chem. Soc.* **1993**, *115*, 9939-9941.
32. Prakash, G. K. S.; Alauddin, M. M.; Hu, J.; Conti, P. S.; Olah, G. A. *J. Labelled Compd. Radiopharm.* **2003**, *46*, 1087-1092.
33. Choi, S. R.; Golding, G.; Zhuang, Z.; Zhang, W.; Lim, N.; Hefti, F.; Benedum, T. E.; Kilbourn, M. R.; Skovronsky, D.; Kung, H. F. *J. Nucl. Med.* **2009**, *50*, 1887-1894.
34. Zhang, W.; Oya, S.; Kung, M.-P.; Hou, C.; Maier, D. L.; Kung, H. F. *Nucl. Med. Biol.* **2005**, *32*, 799-809.
35. Nair, H. K.; Quinn, D. M. *Bioorg. Med. Chem. Lett.* **1993**, *3*, 2619-2622.
36. Tang, W.; Liu, S.; Degen, D.; Ebright, R. H.; Prusov, E. V. *Chem. - Eur. J.* **2014**, *20*, 12310-12319.
37. Darvesh, S.; Kumar, R.; Roberts, S.; Walsh, R.; Martin, E. *Cell. Mol. Neurobiol.* **2001**, *21*, 285-296.
38. Ellman, G. L.; Courtney, K. D.; Andres, V., Jr.; Featherstone, R. M. *Biochem. Pharmacol.* **1961**, *7*, 88-95.
39. Rosenberry, T. L.; Bernhard, S. A. *Biochemistry* **1971**, *10*, 4114-4120.
40. Kelly, C. B.; Mercadante, M. A.; Leadbeater, N. E. *Chem. Commun.* **2013**, *49*, 11133-11148.
41. Imperiali, B.; Abeles, R. H. *Biochemistry* **1986**, *25*, 3760-3767.
42. Allen, K. N.; Abeles, R. H. *Biochemistry* **1989**, *28*, 8466-8473.
43. Wadkins, R. M.; Hyatt, J. L.; Edwards, C. C.; Tsurkan, L.; Redinbo, M. R.; Wheelock, C. E.; Jones, P. D.; Hammock, B. D.; Potter, P. M. *Mol. Pharmacol.* **2007**, *71*, 713-723.
44. Viragh, C.; Harris, T. K.; Reddy, P. M.; Massiah, M. A.; Mildvan, A. S.; Kovach, I. M. *Biochemistry* **2000**, *39*, 16200-16205.
45. Harel, M.; Quinn, D. M.; Nair, H. K.; Silman, I.; Sussman, J. L. *J. Am. Chem. Soc.* **1996**, *118*, 2340-2346.
46. Bourne, Y.; Radic, Z.; Sulzenbacher, G.; Kim, E.; Taylor, P.; Marchot, P. *J. Biol. Chem.* **2006**, *281*, 29256-29267.
47. Radic, Z.; Taylor, P. *J. Biol. Chem.* **2001**, *276*, 4622-4633.

### Highlights

1. Trifluoroacetophenones have high affinities for cholinesterases
2. Chlorodifluoroacetophenones are suitable precursors for trifluoro derivatives
3. Precursors are rapidly converted to trifluoro analogues via F- halogen exchange
4.  $^{18}\text{F}$  incorporation can provide imaging agents for cholinesterases in Alzheimer pathology